Pasanen, Toni P.; von Gastrow, Guillaume; Heikkinen, Ismo T. S.; Vähänissi, Ville; Savin, Hele; Pearce, Joshua

Compatibility of 3-D Printed Devices in Cleanroom Environments for Semiconductor Processing

Published in:
Materials Science in Semiconductor Processing

DOI:
10.1016/j.mssp.2018.08.027

Published: 01/01/2019

Document Version
Peer-reviewed accepted author manuscript, also known as Final accepted manuscript or Post-print

Please cite the original version:
Pasanen, T. P., von Gastrow, G., Heikkinen, I. T. S., Vähänissi, V., Savin, H., & Pearce, J. (2019). Compatibility of 3-D Printed Devices in Cleanroom Environments for Semiconductor Processing. *Materials Science in Semiconductor Processing*, *89*, 59-67. https://doi.org/10.1016/j.mssp.2018.08.027

Compatibility of 3-D Printed Devices in Cleanroom Environments for Semiconductor Processing

T. P. Pasanen[1], G. von Gastrow[1,2], I. T. S. Heikkinen[1], V. Vähänissi[1], H. Savin[1] and J. M. Pearce[1,3,*]

1. Department of Electronics and Nanoengineering, Aalto University, 02150 Espoo, Finland

2. Department of Nanoengineering, University of California San Diego, La Jolla, CA 92093, USA

3. Department of Materials Science & Engineering and Department of Electrical & Computer Engineering, Michigan Technological University, Houghton, MI USA.

* Correspondence: pearce@mtu.edu ; Tel.: +906-487-1466

Keywords: 3-D printing; cleanroom; silicon; semiconductor processing; polymers; particle detection, contamination

Abstract

3-D printing has potential to revolutionize manufacturing of customized low-cost scientific equipment, and numerous self-designed applications have already been realized and demonstrated. However, the applicability of 3-D printed devices to cleanrooms used for semiconductor processing is not as straightforward, as the controlled environment sets strict requirements for the allowed materials and items. This work investigates the opportunity to utilize 3-D printing in cleanrooms by analyzing three potentially suitable polymers (polylactic acid (PLA), acrylonitrile butadiene styrene (ABS) and polypropylene (PP)) for two applications that do not require particular chemical compatibility: a custom single wafer storage box and a wafer positioner for a metrology system. The designed equipment supplements commercial selection by introducing support for samples with non-standard shape or size and simultaneously reduces the price of often extensively expensive cleanroom equipment. The results show that the single wafer boxes 3-D printed from PLA and ABS generate as little particles as a commercial equivalent, whereas slightly more particles are found from a wafer stored in the self-printed PP box. Nevertheless, the number of particles on all wafers is in the same order of magnitude, indicating that 3-D printed boxes are not significant particle sources. The 3-D wafer positioner seems to cause a negligible particle increase on the manipulated wafer, while abrasion of the mechanical parts generate larger numbers of particles that may disperse in the environment. Regular cleaning of those parts is thus recommended, and applicability in a cleanroom environment will depend on the cleanliness constraints. Elemental analysis reveals that 3-D printed objects contain no other harmful metal impurities than those originating from colorants. Thus, 3-D printing filaments with natural color should be preferred for purposes, where metal contamination could be an issue, including semiconductor processing. Finally, 3-D printing filaments considered in this study are shown to be resistant to isopropanol and deionized water, which is critical for efficient cleaning for use of 3-D printed objects in cleanrooms. The results demonstrate that simple 3-D printed objects, such

as wafer boxes or tweezers, are not notable contamination sources, and hence, are equally suitable for use in cleanrooms as the commercial equivalents.

1. Introduction

From the introduction of open source fused filament fabrication (FFF)-based self-replicating rapid prototyper (RepRaP) 3-D printing [1-3], it was clear there was a potential for distributed manufacturing high-quality customized low-cost scientific equipment [4-7]. This potential has been realized where 3-D printed devices are vetted and calibrated for use in a wide variety of scientific fields notably: optics [8,9], microscopy [10,11], biotechnological and chemical labware [12-16] and chemical mixing [15,17,18], colorimeters and turbidimeters [19-21], quartz crystal microbalences [22], liquid autosamplers [23] and fluid handling [24-26], as well as mass spectroscopy equipment [27] and microfluidics [28-32] and medical research [33]. In general, what these devices all have in common is the ability of the user to fabricate exactly the components or complete equipment they need for an experiment as well as reducing the capital cost by 90–99% compared to conventionally produced equipment [5,6,15]. Thus, using open source distributed manufacturing has already created substantial value for the scientific community [34], and tends to make the most sense in limited markets with high markups for scientific tools. Based on these economic factors, RepRap fabricated scientific components would first appear in specialty laboratories.

One notable exception of this rule are cleanrooms used for semiconductor processing. As the dimensions of typical semiconductor devices are in the micrometer range, it is essential to fabricate those components in an environment, where the level of contaminants (e.g. dust particles and organic compounds) is accurately controlled. In cleanrooms, the level of contamination is specified by the number of particles per cubic meter at specified particle sizes by the international ISO (the International Organization for Standardization) standards. The cleanliness classes defined by permitted particle concentrations for different particle sizes are shown in Table 1 according to the ISO 14644-1 standard [35]. To meet these requirements, air flowing into the cleanroom is filtered and constantly recirculated through high-efficiency particulate air (HEPA) filters, and the operators wear protective clothing, including coveralls, a face mask and gloves. The ISO class specifications set limitations also on the materials of cleanroom equipment and tools, including wafer storage boxes and tweezers, as they are allowed to generate only a minuscule amount of particles.

Table 1. ISO classes of cleanroom air cleanliness by particle concentration (5 and 7 used in this study are highlighted)

ISO Class number (N)	Maximum allowable concentrations (particles/m^3) for particles equal to and greater than the considered sizes					
	0.1 μm	0.2 μm	0.3 μm	0.5 μm	1 μm	5 μm
1	10					
2	100	24	10			
3	1000	237	102	35		
4	10000	2370	1020	352	83	
5	**100000**	**23700**	**10200**	**3520**	**832**	
6	1000000	237000	102000	35200	8320	293
7				**352000**	**83200**	**2930**

The use of FFF-based 3-D printing in the cleanroom is limited because of the particles generated during fabrication itself, which depend on numerous factors including filament type, filament color, printing parameters and printer design [36-45]. In addition, the resolution of FFF-based printing limits the technology from making direct contributions in this space. It is currently limited to ~100 micron resolution using thermopolymers, which are deposited in thin layers one after another creating a high surface roughness. In addition, the chemical formulation of low-cost commercial 3-D printing filaments used for the devices above are proprietary (as well as additives such as plasticizers and colorants), which limits the ability to bring in 3-D printed products into the cleanroom due to potential chemical contamination. It is known that metals such as copper and iron have the ability to cause significant, if not catastrophic, harm to semiconductor devices, such as solar cells [46-48] and transistors [49]. It should thus be ensured that those elements are not present in 3-D printed devices meant to be in contact with semiconductors.

Due to the high cost of even basic equipment in cleanrooms, there is thus an opportunity to fabricate customizable alternatives for expensive commercial equipment, but the compatibility with cleanroom conditions, which has extremely strict cleanliness requirements to prevent contamination, has to be first solved. In order to investigate the opportunity to use 3-D printing in cleanrooms, this study analyzes three potentially suitable polymers for the least-strenuous applications in the cleanroom environment – specifically those that do not demand chemical compatibility. Two case studies are used: 1) a custom single wafer storage box and 2) a wafer positioner for a metrology system. Wafer boxes are needed to store wafers securely or to pack them firmly during transportation. However, commercial products are suitable only for full-sized wafers. In research, boxes and holders for various sample sizes are often needed, which cannot be purchased from commercial vendors. Moreover, the commercial wafer boxes are excessively expensive as compared to their function and simplicity. Secondly, there is currently no positioner for accurate placement of samples with non-standard shapes in the metrology system of interest. Thus, the second case study demonstrates the ability to make a bespoke alteration to an existing cleanroom tool.

Commercially and readily available polymers are screened in these two mechanical applications in order to determine requirements to prevent the wear of 3-D printed mechanical parts and prevent particle dissemination. Particle generation of 3-D printed materials is first studied by storing cleaned silicon wafers in 3-D printed wafer boxes. Laser scattering is used for the determination of particle density, as a standard technique for cleanroom air purity measurement [49]. Additionally, the possible effect of mechanical abrasion on particle generation is inspected by operating the custom-made wafer positioner. Since transition metals and several other elements are detrimental for the operation of typical semiconductor devices, the elemental composition of the used 3-D printing filaments is investigated by inductively coupled plasma optical emission spectroscopy (ICP-OES). Finally, chemical resistance of the 3-D printed materials is tested for the most typical and weakest chemicals, namely deionized water and isopropanol.

2. Experimental

2.1 3-D Printing

Three different materials were selected for 3-D printing in this study: polylactic acid (PLA), acrylonitrile butadiene styrene (ABS) and polypropylene (PP). PLA and ABS are the most commonly used materials for 3-D printing [50], and PP is the typical material of commercial cleanroom compatible items [51-53]. Details on the materials are shown in Table 2.

Table 2. 3-D printing materials arranged by nozzle printing temperature

Material	Supplier	Color	Print Temp (°C) at nozzle
Acrylonitrile butadiene styrene (ABS)	IC3D	black	245
Polylactic acid (PLA)	PolyLite	green	205
Polypropylene (PP)	Ultimaker	natural	235

The materials were 3-D printed on a LulzBot TAZ 6 (Aleph Objects). The slicing parameters set for the Cura slicer (https://www.lulzbot.com/cura) are listed on Table 3. All the parts were printed separately. PLA and ABS were printed directly on the printing stage, while for PP, the stage was covered with tape fabricated from the same material to enhance adhesion. After printing the ABS and PLA were removed from the bed mechanically, however the PP was treated with acetone to remove the bottom surface of the tape.

In the case of the wafer positioner, PLA was studied rather than other materials such as PP and ABS. PLA it is the most convenient material in terms of printing quality, as it does not cause warping, and is also the most common plastic for 3-D printing.

Table 3. Slicing settings used to print the wafer boxes

Parameter	ABS	PLA, wafer boxes	PLA, wafer positioner	PP
Quality • Layer height (mm) • Shell thickness (mm)	 0.22 1.0	 0.25 1.0	 0.20 1.0	 0.18 1.0
Fill • Bottom/top thickness (mm) • Fill density (%)	 1.1 20	 1 20	 1 20	 1.08 20
Speed and temperature • Print speed (mm/s) • Printing temperature (C) • Bed temperature (C)	 50 245 95	 50 205 60	 50 210 60	 50 235 60
Support • Support type • Platform adhesion type	 None None	 None None	 None None	 None Brim
Filament • Diameter (mm) • Filament flow (%)	 2.85 100	 2.85 100	 2.85 90	 2.85 90
Nozzle size	0.5	0.5	0.5	0.5
Retraction • speed (mm/s) • distance (mm)	 10 1	 10 1.75	 10 1	 10 1
Quality • Initial layer thickness (mm) • Initial layer line width (%) • Cut off object bottom (mm)	 0.425 125 0.0	 0.425 125 0.0	 0.425 125 0.0	 0.425 125 0.0
Speed • Travel speed (mm/s) • Bottom layer speed (mm/s) • Infill speed (mm/s) • Top/bottom speed (mm/s) • Outer shell speed (mm/s) • Inner shell speed (mm/s)	 175 15 55 45 45 50	 175 15 50 40 40 45	 175 15 50 40 40 45	 175 10 60 10 10 60
Minimal layer time (sec)	15	30	10	15

2.2 Particle Generation

The number of particles with specific sizes were first measured on 150 mm diameter wet-chemically oxidized clean silicon wafers with NanoPhotonics Reflex TT wafer defect inspection system. The equipment illuminates the surface of a rotating wafer with a diode laser and determines the number of particles based on the back-scattered light [54]. Five Si wafers were then stored in an ISO 5 class cleanroom under a HEPA filter inside the following single wafer boxes (Fig. 1):

a. No box
b. Commercial box (Fluoroware Inc., natural PP)
c. 3-D printed box (green PLA)
d. 3-D printed box (black ABS)
e. 3-D printed box (natural PP)

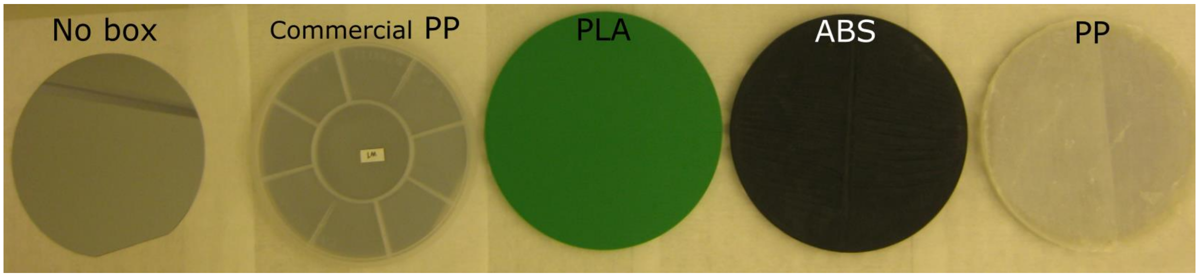

Figure 1. Wafers under storage. From left to right: wafer with no box, commercial PP, 3-D printed PLA, 3-D printed ABS, and 3-D printed PP.

All boxes were wiped with dust-free cleanroom compatible wipes (Quiltec, 2-ply polyester) and isopropanol (IPA) prior to storage, and the boxes were kept a lid closed during the whole storage time. Additionally, one wafer was stored on a cleanroom paper without a box for reference. The number of particles on each wafer was re-measured after 15 days. The wafer storage test was performed twice with identical procedure to increase reliability of the data.

Different locations of the positioner printed in PLA were tested for particle generation, which was suspected to originate mostly from the mechanical parts. Silicon wafers were placed in the vicinity of the printed devices on a table under cleanroom air flow and used to determine the number of generated particles in a given amount of time. Reference wafers were placed in the same environment without the wafer positioner. Particle measurements were performed on the wafers prior to the experiment and after four and 27 days using the same method as previously explained. After the measurements at day 1 and day 4, the gear was moved 25 times along the whole graduated axis to simulate device operation. The cleanroom airflow was used to disperse the generated particles over the wafer until the next measurement. One wafer was placed under the device to collect particles originating from abrasion due to the movement of the mechanical parts, and another wafer was placed in the clamp to mimic an actual case of wafer positioning, as depicted in Figure 2. Measurements were performed on those wafers both for devices placed in ISO 5 and ISO 7 cleanroom areas. The measurement uncertainties were obtained from the standard deviation of five measurements repeated on a wafer.

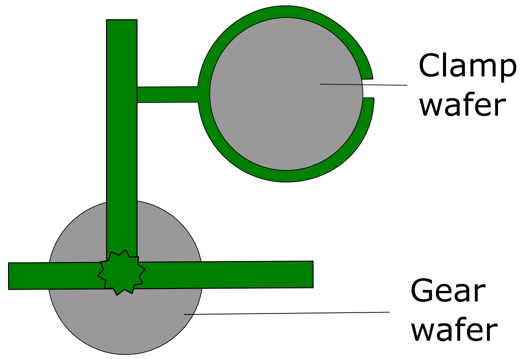

Figure 2. Schematic of the measurement setup for the wafer positioner

2.3 Elemental composition of 3-D printed objects

To ensure that no deleterious contaminating materials, such as noble or trace metals, are released from the 3-D printed boxes on the wafers during storage and possible scratching, elemental composition in pieces of each printed material was determined by inductively coupled plasma optical emission spectroscopy (ICP-OES) and atomic absorption spectroscopy (AAS). A piece of commercial PP storage box was also inspected similarly. The samples were wiped with dust-free wipes and IPA prior to characterization and handled with clean nitrile gloves. They were melted in heated sulfuric acid, and nitric acid was added to the solution after approximately six hours of heating to fully disintegrate the polymers. The concentration of K and Na was determined by AAS and that of Ag, Al, Au, Ca, Co, Cr, Cu, Fe, Hg, Mg, Mn, Ni, Ti, and Zn by ICP-OES from all samples (Fassel, 1974).

2.4 Chemical resistance

To reduce the number of particles entering a cleanroom, all items, which have been outside the controlled environment, typically need to be wiped with a dust-free wipe moistened with deionized water (DIW) and IPA in the cleanroom airlock. Therefore, it is essential that 3-D printed materials tolerate these chemicals. The chemical resistance of the selected 3-D printing materials (i.e., PLA, ABS and PP) for DIW and IPA were hence inspected by immersing samples of the plastics in the solvents for one week and observing changes in their mass and dimensions afterwards.

First, 20-25 mm long pieces of filament were cut from the spools with IPA-cleaned scissors. Also 3-D printed samples (dimensions 23 mm x 6 mm x 2 mm) were prepared from the same filaments with same printing parameters as described earlier (see the wafer box parameters for PLA in Table 3) with the exception of 100 % infill. All samples were weighed with a precision scale (VWR, accuracy ±0.001 g), and the diameter of the filaments and the dimensions of the printed samples were measured using a digital caliper (accuracy ±0.01 mm). Samples were handled with gloves on to prevent contamination from skin.

The samples were put into borosilicate glass vials (clear Wheaton 4 ml, styrene-butadiene caps) with plastic tweezers, and the solvents were added into the vials with plastic LD-PE pipettes to fully immerse the samples. The vials were closed and stored inside a fume hood for one week, after which the samples were rinsed with DIW and dried with a nitrogen gun. To make sure that all solvent had evaporated from the immersed samples, they were placed in a vacuum drying oven for four days, after which they were measured and weighed with the same tools as in the beginning.

3. Results and Discussion

3.1 Case study 1: Single Wafer Box

Single wafer boxes are typically used to pack wafers firmly (e.g., during shipping or to store valuable samples securely). Commercial boxes (e.g. https://www.sps-europe.com/order/4enquot-100mm-coin-style-single-wafer-shipper/15131/ or http://www.wafercare.com/page.aspx?id=35) are readily available for nearly all commonly-used wafer sizes used in semiconductor processing. However, the commercial products are designed only for full wafers, and in some occasions, especially in research-scale processing, smaller samples, such as wafer quarters, are used for convenience and to reduce material costs [56-59]. As the commercial products have a support for samples only at the edges, wafer quarters lie on the bottom of the box at the center and can freely move in the box, which causes mechanical damage and scratching of the samples. Single wafer boxes that would be suitable for smaller samples are not available from commercial vendors, since their operation relies on mass production of certain products for the largest markets.

This work demonstrates a fully 3-D printable and customizable single wafer box. As an example, the box is designed for four 100 mm wafer quarters. The design consists of three separate parts, which can be 3-D printed separately or in one run and are shown in Fig. 3a: a bottom (blue, bottom right), a lid (black, bottom left) and a spider spring (top). The rendering of the bottom part of the design is provided for clarity in Fig. 3b, which shows additional features compared to commercially-available wafer boxes. In addition to the raised bottom at the edges, the box has sample supports also in the center to ensure horizontal position of the samples. Furthermore, the sample separator walls in the center and the edges prevent the quarters from sliding on top of each other as shown with wafer quarters held in Fig. 3c. This helps to avoid sample scratching, unlike in the commercial boxes, where wafer pieces can freely move and impact one another (Fig. 3d). Scratching is detrimental for nearly all semiconductor materials and devices, which typically have micro- or nanometer scale features, and especially for e.g. nanostructured black silicon surfaces (as shown in Figs. 3c and 3d as an example), which are damaged extremely easily. In addition, the box has a spider spring to prevent vertical movement of the samples and a locking mechanism for the lid, which are both found also in the commercial products. The back side of the box bottom has a groove matching with front edge, which enables stacking of several boxes firmly. Finally, the samples can be easily removed with tweezers due to a gap in the outer support.

The customizable open-source OpenSCAD design, as well as ready-to-print stl files, can be found from https://3dprint.nih.gov/discover/3dpx-008323. The size of the box can easily be tuned for various wafer sizes by changing only one parameter in the .scad code. Additionally, the sample separators can be modified to support different wafer piece sizes (e.g. wafer halves or smaller samples instead of quarters). Furthermore, all the parameters, including thickness of the bottom and the walls and tolerances for wafer size, can be conveniently changed using dedicated variables. This allows users to customize the box for their specific printer, filament type and application.

Furthermore, the 3-D printed box is three to four times less expensive than the commercial equivalents. The cost of the printed components is \$0.90, \$0.40 and \$0.025 for the bottom, lid, and spider spring parts (or \$1.33 / complete box), estimated by the Cura slicing software (https://www.lulzbot.com/cura) and based on a price of commercial filament of \$25 per 1 kg of PolyLite PLA (https://www.lulzbot.com/store/filament/polylite-pla), whereas commercial equivalents cost around \$5 when ordered in large quantities (quotation for http://www.wafercare.com/page.aspx?id=35 from a Finnish importer Tecalemit Flow Oy).

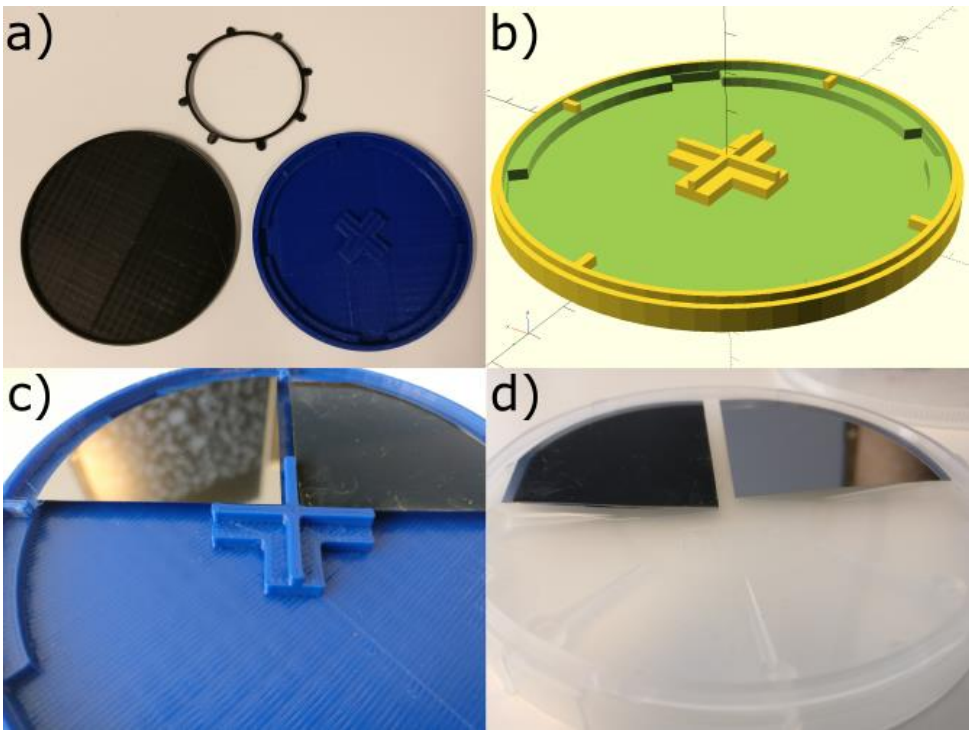

Figure 3. a) Wafer box for four 100 mm wafer quarters 3-D printed out of PLA including top (black), bottom (blue) and holder (black ring). b) Open SCAD model of the customizable single wafer box. c) Wafer quarters stored securely in the 3-D printed box. d) Wafer quarters free to move in a commercial single wafer box.

3.2 Case study 2: Wafer Positioner

This section presents a customized positioner for semiconductor wafers. It aims at improving the localization of measurements to allow their repeatability at identical sample locations, which can be difficult with samples of arbitrary shapes. It can also be required to perform successive measurements at different sample locations, where a certain distance is required between single measurement points to ensure that the subsequent measurements do not interfere with each other. Sample positioning must often be performed on an already-existing measurement stage, and for that reason an external device should be used rather than a full-sized moveable stage that could interfere with the measurement. Examples of applications where this functionality is useful include Kelvin Probe and ellipsometry measurements, and they are not limited to equipment inside cleanrooms.

The positioner showed here has been specifically developed for the Semilab PV2000 semiconductor characterization tool [60]. The measurement stage is metallic and must be electrically conductive. For that reason, the positioner has to be designed in such a way that it does not support the sample.

The device consists in a primary rail that includes a rack and pinion to allow displacement in the X-direction. A secondary rail is attached to the rack and the sample clamp can move along this rail for displacement in the Y-direction. Figure 4a presents the different modelled parts of the device, and a photo of the assembled device is shown in Fig. 4b. Note that a new clamp can easily be printed separately to adapt to different sample geometries.

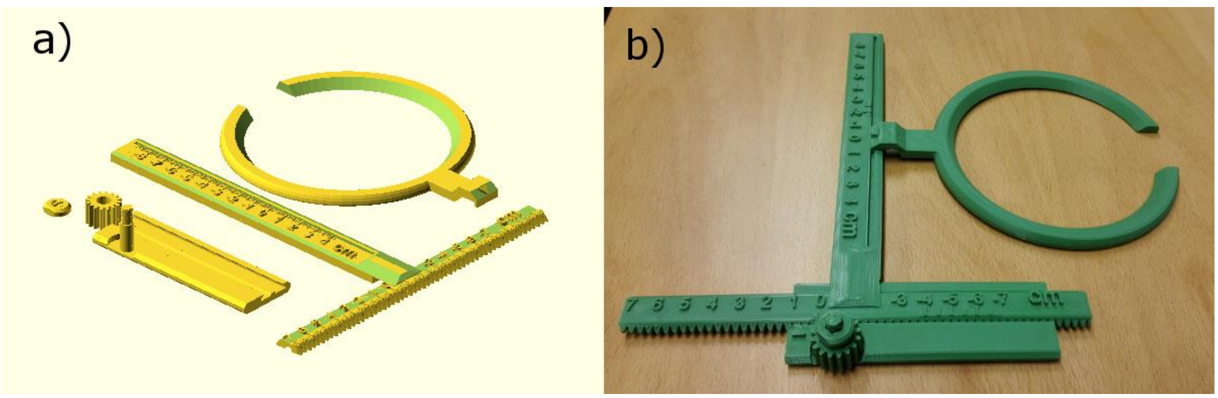

Figure 4: a) Parts of the positioner modelled in the OpenSCAD software. b) 3-D printed and assembled positioner.

The .stl and .scad files can be found at https://3dprint.nih.gov/discover/3dpx-008207. The price of a PLA-printed device is estimated at $1.30 based on a cost of $25/kg for PLA.

3.3 Particle generation

3.3.1 Single Wafer Boxes

In order to avoid airborne particles from being adsorbed on wafer surfaces, wafers are typically stored inside plastic boxes. However, although a properly sealed box provides efficient protection against airborne particles, the box itself may act as a source of contamination, since organic additives in the plastic materials may adsorb on the stored wafers [52,61]. Hence, in a cleanroom environment with extremely low airborne particle concentration (Table 1), the amount of adsorption is minimized by storing wafers with no cover. Indeed, Fig. 5 shows that the least particles are adsorbed on wafers stored with no box under a HEPA filter compared to wafers stored in any of the inspected boxes, including the commercial ones. Similar storage in cleanroom air with no cover has been shown to have no or only little effect on the surface recombination velocity of such surfaces, especially when the surfaces are protected with a thin wet chemical oxide [62].

However, due to practical reasons and the high cost of cleanroom space [63], wafers generally need to be stored in boxes inside cleanrooms.

Figure 5 shows that particle generation of all 3-D printed single wafer boxes is in the same order of magnitude compared to the commercial equivalent, which is commonly used in cleanrooms. Closer inspection reveals that wafer boxes 3-D printed from ABS and PLA outperform the commercial PP box. Both of them generate slightly less particles than the commercial reference, apart from the range of smallest particles with less than 2 μm size, where the particle count on a wafer stored in the PLA box slightly exceeds that of the commercial PP box. However, the 3-D printed PP box generates more small particles than the commercial equivalent. This is most likely due to the remaining sticky tape on the outer surface, which was used to enhance adhesion to the printing bed, although most of the glue was dissolved in acetone directly after the printing. Nevertheless, the 3-D printed PP box generates less large particles than the commercial PP box and is nearly as good as the other 3-D printed boxes. However, the largest particles are likely caused by wafer handling with tweezers, and hence, may not directly reflect the particle generation of the wafer boxes. From the particle generation point of view, the 3-D printed boxes appear equally suitable for cleanroom environments as the commercial equivalent.

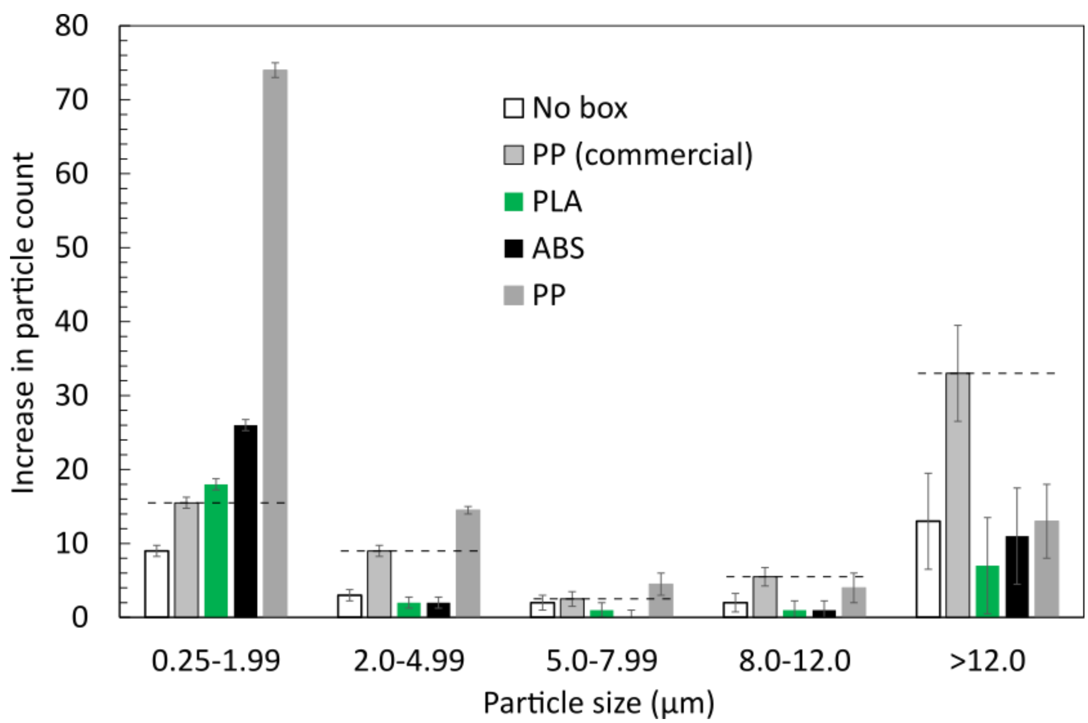

Figure 5. Increase in particle count during 15 days storage in various single wafer boxes. The initial number of particles on all wafers were in the order of 10-20. The dashed lines indicate reference levels set by the commercial PP box, which is commonly used in cleanroom environments. The error bars are determined from the variation in several repeated measurements.

3.3.2 Wafer positioner

While the tests performed on 3-D printed wafer boxes resulted in a low density of emitted particles, they do not reflect particle emission caused by moving parts. More generally, the issue of particle generation via abrasion in 3-D printed materials is of paramount importance in view of cleanroom applications. This was studied with the help of the wafer positioner presented in Section 3.2.

Figure 6a shows the increase of particles at each location in the wafer positioner with respect to the initial particle count. Figure 6b shows the particle distribution after each measurement on a wafer placed inside the positioner clamp in an ISO 5 area. Most particles have a diameter smaller than 2 µm, which complies with cleanroom limits, as shown in Table 1. Note that particle distributions were similar for all measurements performed in this study.

As reported in Fig. 6a, the number of particles generated under the gear of the wafer positioner is similar in the ISO 5 and ISO 7 areas (~200 particles generated in 27 days, using the reference wafers as baselines). This hints that the stronger air flow in the ISO 5 area did not cause a wider (and thus more detrimental for the cleanroom) dispersion of the particles, as it would have resulted in a smaller increase in the number of measured particles on the wafer. Figure 5a illustrates that the harm caused by particle increase will depend on the target application and on the cleanroom cleanliness standard. In the ISO 7 cleanroom, the number of particles generated in 27 days near the gear was 25 % higher than that in the reference wafer (1028 against 840), while this number rises to 600 % in the ISO 5 cleanroom (288 against 41) due to the very low baseline level of particle contamination.

However, the number of particles generated near the wafer clamp is the most relevant data as it reflects true device operation. It is closer to the number of particles generated in the reference wafer (particle increase of 119 near the clamp against an increase of 41 particles the reference wafer after 27 days). After four days, only 44 particles have been generated on a wafer placed in the positioner clamp in the ISO 5 area (against 0 in the reference). As can be seen in Fig. 5a, the particle increase near the 3-D printed positioner clamp is in the same range as that on a wafer stored in a commercial box.

In conclusion, it seems that normal operation of the positioner would cause a limited increase of the number of particles on the measured wafer. There seems to be a higher increase near mechanical parts due to abrasion, which may however be insignificant for applications that do not require to maintain a remarkably high level of cleanliness in the environment (as opposed to photolithography and high-temperature anneal areas, for instance). The next section will investigate the chemical nature of the generated particles in order to determine their potential harmfulness.

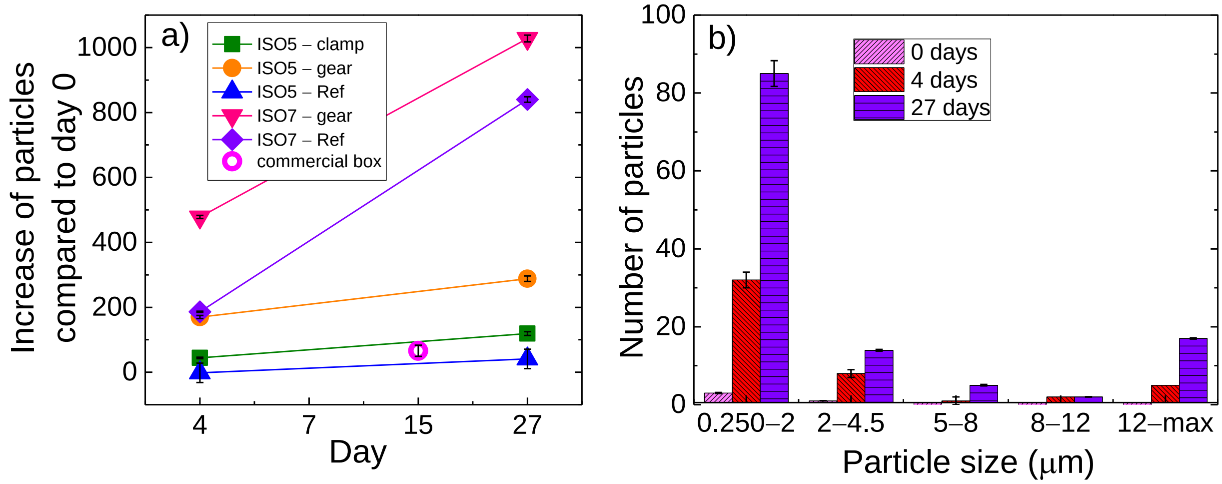

Figure 6. Particle generation results obtained with the PLA 3-D printed wafer positioner. Figure a) displays the increase of particles compared to the initial value for each location in the wafer positioner (wafer clamp and ruler gear) and different cleanroom areas. The particle increase on a wafer stored in a commercial box is given for comparison. Figure b) shows the particle distribution after each measurement for a wafer placed inside the clamp in the ISO 5 area.

3.4 Elemental analysis

Figure 7 presents concentrations of different metals in the substance of commercial PP wafer boxes and 3-D printed PLA, ABS, and PP. Concentration of most elements (Ag, Au, Co, Cr, Cu, Fe, Hg, Mg, Mn, Ni, and Zn) is below the detection limit of 50 µg/g for ICP-OES. This amount of any of the inspected impurities in the adsorbed particles would result in negligible contamination in silicon wafers. However, since the majority of the mass is concentrated in the largest particles, the possibility of minor spot-like contamination is not excluded.

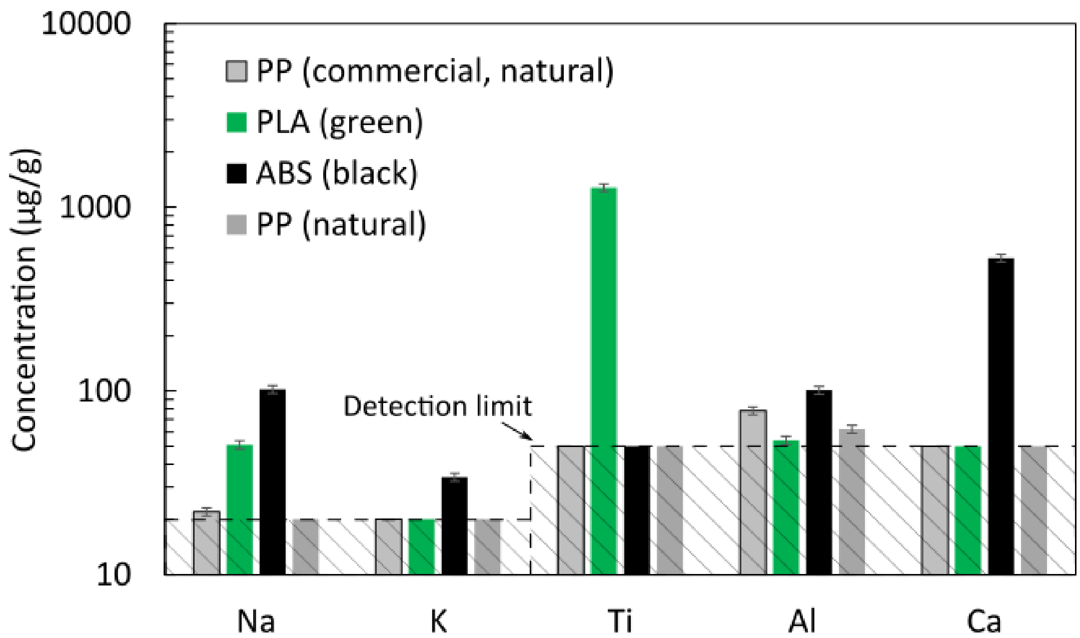

Figure 7. Concentrations (µg/g) of five metals in pieces of 3-D printed materials. A piece of commercial PP wafer box is included for reference. Detection limits of ICP-OES and AAS are 50 µg/g and 20 µg/g, respectively. Concentrations of Ag, Au, Co, Cr, Cu, Fe, Hg, Mg, Mn, Ni, and Zn were below the detection limits in all inspected materials. Note the logarithmic y-axis. The error bars have been estimated based on a 5 % inaccuracy in the measured concentration.

The commercial and 3-D printed PP, both of which contain no intentionally-added colorants, show similar metal contents. More accurately, Al concentration in the commercial box substance is slightly higher than that of the 3-D printed equivalent, which indicates that the 3-D printed PP box is at least equally cleanroom compatible as the commercially available products from contamination perspective.

The amount of Al in the other two 3-D printed materials inspected in this study (i.e., PLA and ABS) is comparable to that in both PP boxes. However, PLA and ABS also contain a notable amount of one or more other metals: Na is found from both samples, Ti is detected in PLA, and K and Ca in ABS. Nevertheless, all of the detected metals are common colorants in plastics [64,65], which explains the presence of those elements in the inspected samples. Hence, 3-D printing filaments with natural color (i.e., without colorants) should be preferred for purposes, where metal contamination could be an issue, including semiconductor processing in cleanroom environments [66,67].

3.5 Chemical resistance

Figure 8 presents the relative changes in mass and dimensions of PLA, ABS, and PP samples in DIW and IPA. The immersion causes only small, less than 0.5 % and 2 % changes in mass and dimensions of all samples, respectively, and no interlayer delamination is observed in the 3-D printed pieces.

Dimensions of the PLA pieces, both filament and 3-D printed, increase with approximately 1 % in both DIW and IPA, indicating that the polymers have absorbed a small amount of liquid during immersion. However, the sample masses remain constant, which denotes that the absorbed solvent has evaporated in vacuum drying oven and the plastic has become more porous.

ABS filament shows slightly larger change in sample dimensions than PLA when immersed in DIW. However, the dimensions of a 3-D printed piece of the same material decrease in DIW, suggesting that the sample is slightly dissolving in the liquid. In IPA, nevertheless, similar dissolution is not observed, as both mass and diameter of ABS samples remain unchanged. DIW and IPA have the least effect on PP. The dimensions of the PP filament piece only slight increase and those of the 3-D printed PP sample decrease in IPA. Nevertheless, the change is insignificant considering the measurement accuracy.

In general, the negligibly small changes in the mass and diameter of the 3-D printed samples demonstrate that 3-D printed objects can be cleaned with a wipe moistened with DIW or IPA without affecting the properties of the printed items, which enables bringing the objects securely into a cleanroom. A more comprehensive study on the chemical stability of 3-D printed materials can be found elsewhere [68].

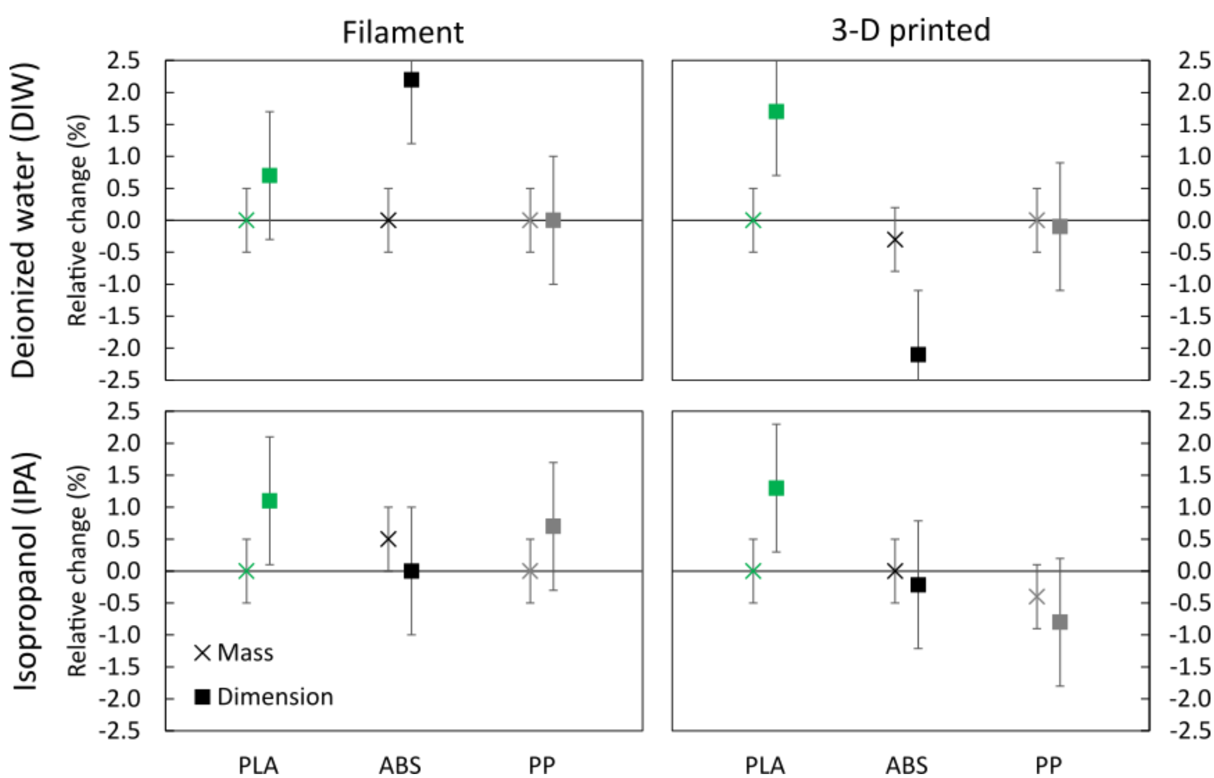

Figure 8. Relative change in mass and diameter of PLA, ABS, and PLA filaments and corresponding 3-D printed samples in deionized water (DIW) and isopropanol (IPA). The error bars have been estimated based on 0.5 % and 1.0 % inaccuracy in mass and dimension, respectively.

After confirming the chemical resistance and the absence of metal impurities in 3-D printed objects, the subsequent step would be to extend the use of 3-D printed equipment to more demanding cleanroom applications. These include jigs used in wafer cleaning prior to thermal oxidation, where even minuscule contamination may have detrimental consequences, or parts of semiconductor processing equipment, such as atomic layer deposition chamber. Both applications require extreme resistance to harsh environments, which sets yet more stringent requirements to the filament materials and the 3-D printing technology, and needs to be addressed in future studies.

4. Conclusions

This work investigated the applicability of 3-D printed equipment to cleanroom environments via two example applications: a custom wafer storage box and a wafer positioner for a metrology system. The custom-made single wafer box fulfilled the gap in commercial wafer box selection to secure small samples, e.g. wafer quarters, firmly. The wafer positioner enabled accurate placement of samples with non-standard shapes on the measurement stage of a metrology system.

The single wafer boxes 3-D printed from PLA and ABS generated equal number of particles as the commercial equivalent. However, particle generation from the self-printed PP box was slightly higher, which was most likely due to challenges in removing the tape used to enhance adhesion to the printing bed. The 3-D wafer positioner is a unique piece of equipment; thus no commercial equivalent exists for comparison purposes. Comparison with the wafer boxes indicated that, for normal operation of the positioner (wafer placed inside the clamp), particle generation was in the same range as in commercial and 3-D-printed wafer boxes. More particles are generated near the mechanical parts and can diffuse in the environment, thus regular cleaning of those part is recommended.

Elemental analysis on pieces of 3-D printed filaments revealed that the printed materials are in general free of detrimental metal contamination, other than those introduced by colorants. Thus, 3-D printing filaments with natural color should be preferred for purposes, where metal contamination could be an issue, including semiconductor processing. Additionally, 3-D printing filaments were found to be resistant to isopropanol and deionized water, which is used for cleaning objects before bringing them into a cleanroom. The results demonstrate that 3-D printed objects, such as wafer boxes, tweezers or wafer positioners, fulfill the strict particle generation requirements set for items used in cleanrooms. Hence, it can be concluded that 3-D printing enables manufacturing of customized low-cost scientific equipment even in special laboratory environments such as cleanrooms.

5. Acknowledgements

This project was supported by Fulbright Finland. The authors acknowledge the provision of facilities and technical support by Aalto University at OtaNano – Micronova Nanofabrication Centre. T. P. Pasanen acknowledges the Aalto ELEC Doctoral School, Jenny and Antti Wihuri Foundation, and Walter Ahlström Foundation for the financial support.

6. References

1. Sells, E., Bailard, S., Smith, Z., Bowyer, A., Olliver, V. (2010). RepRap: the replicating rapid prototyper-maximizing customizability by breeding the means of production. *Proceedings in the World Conference on Mass Customization and Personalization,* Cambridge, MA, USA, 7-10 October 2007.
2. Jones, R., Haufe, P., Sells, E., Iravani, P., Olliver, V., Palmer, C., Bowyer, A. (2011). RepRap-the replicating rapid prototyper. *Robotica* 29 (01): 177–91.
3. Bowyer, A. (2014). 3D printing and humanity's first imperfect replicator. *3D Printing and Additive Manufacturing 1* (1): 4–5.
4. Pearce, J. (2012). Building research equipment with free, open-source hardware. *Science*, *337* (3100): 1303–4.
5. Pearce, J. (2014). *Open-source lab: how to build your own hardware and reduce research costs*, 1st ed. Elsevier: Waltham, MA, USA.
6. Pearce, J.M (2014). Laboratory equipment: cut costs with open-source hardware. *Nature*, 505 (7485) 618-618
7. Coakley, M. and Hurt, D.E. (2016). 3D printing in the laboratory maximize time and funds with customized and open-source labware. *Journal of Laboratory Automation*, p.2211068216649578.
8. Zhang, C., Anzalone, N.C., Faria, R.P., Pearce, J.M. (2013) Open-source 3D-printable optics equipment. *PLoS ONE* 8(3): e59840. doi:10.1371/journal.pone.0059840
9. Salazar-Serrano, L.J., Valencia, A. and Torres, J.P. (2016) A 3D printed toolbox for opto-mechanical components. *arXiv preprint* arXiv:1606.09563.
10. Sharkey, J.P., Foo, D.C., Kabla, A., Baumberg, J.J. and Bowman, R.W. (2016) A one-piece 3D printed flexure translation stage for open-source microscopy. *Review of Scientific Instruments*, 87(2), p.025104.
11. Wijnen, B., Petersen, E. E., Hunt, E. J. and Pearce, J. M. (2016), Free and open-source automated 3-D microscope. *Journal of Microscopy* 264(2), 238-246. doi:10.1111/jmi.12433
12. B.C. Gross, J.L. Erkal, S.Y. Lockwood, C. Chen, D.M. Spence (2014). Evaluation of 3D printing and its potential impact on biotechnology and the chemical sciences. Analytical Chemistry 86 (7):3240-3253
13. T.H. Lücking, F. Sambale, S. Beutel, T. Scheper (2014). 3D-printed individual labware in biosciences by rapid prototyping: in vitro biocompatibility and applications for eukaryotic cell cultures. *Engineering Life Science* 15 (1):. 57-64
14. Su, C.-K., Hsia, S.-C., Sun, Y.C. (2014). Three-dimensional printed sample load/inject valves enabling online monitoring of extracellular calcium and zinc ions in living rat brains. *Analytica Chimica Acta*, 838 : 58-63.
15. Baden, T., Chagas, A., Marzullo, T., Prieto-Godino, L., Euler, T. (2015). Open labware: 3-D printing your own lab equipment. *PLoS Biology 13* (3).
16. T.R. Damase, D. Stephens, A. Spencer, P.B. Allen (2015) Open source and DIY hardware for DNA nanotechnology labs. *Journal of Biological Methods*, 2 (3) p. e24.
17. Dhankani, K., Pearce, J. M. (2017). Open source laboratory sample rotator mixer and shaker. *HardwareX* 1, 1-12.

18. Trivedi, D. K., & Pearce, J. M. (2017). Open source 3-D printed nutating mixer. *Applied Sciences*, *7*(9), 942.
19. Anzalone, G. C., Glover, A. G., & Pearce, J. M. (2013). Open-source colorimeter. *Sensors*, *13*(4), 5338-5346.
20. Wijnen, B., Anzalone, G.C. and Pearce, J.M. (2014). Open-source mobile water quality testing platform. *Journal of Water Sanitation and Hygiene for Development*, 4(3):532-537.
21. Kelley, C. D., Krolick, A., Brunner, L., Burklund, A., Kahn, D., Ball, W. P., & Weber-Shirk, M. (2014). An affordable open-source turbidimeter. *Sensors*, *14*(4), 7142-7155.
22. Mista, C., Zalazar, M., Peñalva, A., Martina, M. and Reta, J.M., (2016). Open source quartz crystal microbalance with dissipation monitoring. In *Journal of Physics: Conference Series* (Vol. 705, No. 1, p. 012008).
23. Carvalho, M.C., Eyre, B.D. (2013). A low cost, easy to build, portable, and universal autosampler for liquids. *Methods Oceanography*., 8: 23-32
24. Wijnen, B., Hunt, E. J., Anzalone, G. C., & Pearce, J. M. (2014). Open-source syringe pump library. *PloS One*, *9*(9), e107216.
25. Zhang, C., Wijnen, B., & Pearce, J. M. (2016). Open-source 3-D platform for low-cost scientific instrument ecosystem. *Journal of Laboratory Automation*, *21*(4), 517-525.
26. Bravo-Martinez, J. (2018). Open source 3D-printed 1000 µL micropump. *HardwareX* 3: 110-116.
27. Maldonado-Torres, M., López-Hernández, J.F., Jiménez-Sandoval, P. and Winkler, R., (2014). ‘Plug and Play’assembly of a low-temperature plasma ionization mass spectrometry imaging (LTP-MSI) system. *Journal of Proteomics*, 102, 60-65.
28. He, Y., Qiu, J., Fu, J., Zhang, J., Ren, Y., & Liu, A. (2015). Printing 3D microfluidic chips with a 3D sugar printer. *Microfluidics and Nanofluidics*, *19*(2), 447-456.
29. Pearce, J. M., Anzalone, N. C., & Heldt, C. L. (2016). Open-source wax RepRap 3-D printer for rapid prototyping paper-based microfluidics. *Journal of Laboratory Automation*, *21*(4), 510-516
30. White, J. A., & Streets, A. M. (2018). Controller for microfluidic large-scale integration. *HardwareX 3, 135-145*
31. Brower, K., Puccinelli, R.R., Markin, C.J., Shimko, T.C., Longwell, S.A., Cruz, B., Gomez-Sjoberg, R. and Fordyce, P.M., (2018). An open-source, programmable pneumatic setup for operation and automated control of single-and multi-layer microfluidic devices. *HardwareX*, 3,117-134.
32. Gaal, G., Mendes, M., de Almeida, T. P., Piazzetta, M. H., Gobbi, Â. L., Riul, A., & Rodrigues, V. (2017). Simplified fabrication of integrated microfluidic devices using fused deposition modeling 3D printing. *Sensors and Actuators B: Chemical*, *242*, 35-40.
33. Niezen, G., Eslambolchilar, P. and Thimbleby, H., (2016). Open-source hardware for medical devices. *BMJ Innovations*, 2:78-83
34. Pearce, J.M. (2016). Return on investment for open source scientific hardware development. *Science and Public Policy*, 43 (2): 192-195
35. ISO 14644-1:2015. Cleanrooms and associated controlled environments. Part 1: Classification of air cleanliness by particle concentration.
36. Deng, Y., Cao, S. J., Chen, A., & Guo, Y. (2016). The impact of manufacturing parameters on submicron particle emissions from a desktop 3D printer in the perspective of emission reduction. *Building and Environment*, 104, 311-319.

37. Kim, Y., Yoon, C., Ham, S., Park, J., Kim, S., Kwon, O., & Tsai, P. J. (2015). Emissions of nanoparticles and gaseous material from 3D printer operation. *Environmental science & technology*, *49*(20), 12044-12053.
38. Kwon, O., Yoon, C., Ham, S., Park, J., Lee, J., Yoo, D., & Kim, Y. (2017). Characterization and control of nanoparticle emission during 3D printing. *Environmental Science & Technology*, 51(18), 10357-10368.
39. Stabile, L., Scungio, M., Buonanno, G., Arpino, F., & Ficco, G. (2017). Airborne particle emission of a commercial 3D printer: the effect of filament material and printing temperature. *Indoor Air*, 27(2), 398-408.
40. Azimi, P., Fazli, T., & Stephens, B. (2017). Predicting concentrations of ultrafine particles and volatile organic compounds resulting from desktop 3D printer operation and the impact of potential control strategies. *Journal of Industrial Ecology* 21(S1), S107-S119.
41. Weber, R. J., Zhang, Q., Wong, J. P., Davis, A., & Black, M. (2016). Fine particulate and chemical emissions from desktop 3D printers. In *NIP & Digital Fabrication Conference* (Vol. 2016, No. 1, pp. 121-123). Society for Imaging Science and Technology.
42. Floyd, E. L., Wang, J., & Regens, J. L. (2017). Fume emissions from a low-cost 3-D printer with various filaments. *Journal of Occupational and Environmental Hygiene*, 14(7), 523-533.
43. Stefaniak, A.B., LeBouf, R.F., Yi, J., Ham, J., Nurkewicz, T., Schwegler-Berry, D.E., Chen, B.T., Wells, J.R., Duling, M.G., Lawrence, R.B. and Martin Jr, S.B., (2017). Characterization of chemical contaminants generated by a desktop fused deposition modeling 3-dimensional Printer. *Journal of Occupational and Environmental Hygiene*, 14(7), 540-550.
44. Vance, M. E., Pegues, V., Van Montfrans, S., Leng, W., & Marr, L. C. (2017). Aerosol emissions from fuse-deposition modeling 3D printers in a chamber and in real indoor environments. *Environmental Science & Technology*, 51(17), 9516-9523.
45. Zhang, Q., Wong, J. P., Davis, A. Y., Black, M. S., & Weber, R. J. (2017). Characterization of particle emissions from consumer fused deposition modeling 3D printers. *Aerosol Science and Technology*, 51(11), pp.1275-1286.
46. Bemski, G. (1958). Recombination properties of gold in silicon. *Physical Review*, 111(6), 1515.
47. Gill, A. A., Baber, N., & Iqbal, M. Z. (1990). Role of the mid-gap level as the dominant recombination center in platinum doped silicon. *Journal of Applied Physics*, 67(2), 1130-1132.
48. Lindroos, J., Yli-Koski, M., Haarahiltunen, A., Schubert, M. C., & Savin, H. (2013). Light-induced degradation in copper-contaminated gallium-doped silicon. *Physica Status Solidi (RRL)-Rapid Research Letters*, 7(4), 262-264.
49. Franssila, S. (2004). *Introduction to Microfabrication*, 2nd edition, John Wiley & Sons, ISBN: 978-0-470-74983-8.
50. Wohlers, T. (2016). *Wohlers Report 2016*. Wohlers Associates, Inc., Fort Collins, Colorado, USA.
51. Hattori, T. (1997). Key Issues in wet chemical cleaning of silicon surfaces. *In the 1997 ECS & ISE Joint International Meeting*, 2133.

52. Saga, K. & Hattori, T. (1996). Identification and removal of trace organic contamination on silicon wafers stored in plastic boxes. *Journal of The Electrochemical Society*, 143(10), 3279-3284.
53. Budde, K. J., Holzapfel W. J., & Beyer M. M. (1995). Application of ion mobility spectrometry to semiconductor technology: outgassings of advanced polymers under thermal stress. *Journal of The Electrochemical Society*, 142(3), 888-897.
54. Lilienfeld, P. (1986). Optical detection of particle contamination on surfaces: a review. *Aerosol Science and Technology* 5(2), 145-165.
55. Fassel, V. A. & Kniseley, R. N. (1974) Inductive coupled plasma – optical emission spectroscopy. *Analytical Chemistry* 46 (13): 1110-1120.
56. McCamey, D. R.; Francis, M.; McCallum, J. C.; Hamilton, A. R.; Greentree, A. D., & Clark, R. G. (2005). Donor activation and damage in Si–SiO2 from low-dose, low-energy ion implantation studied via electrical transport in MOSFETs. *Semiconductor Science and Technology* 20, 363–368.
57. Grant, N. E.; Markevich, V. P.; Mullins, J.; Peaker, A. R., Rougieux, F., & Macdonald, D. (2016). Thermal activation and deactivation of grown-in defects limiting the lifetime of float-zone silicon. *Physica Status Solidi – Rapid Research Letters*, 10 (6) 443-447.
58. Balakrisnan, B.; Patil, S., & Smela, E. (2009). Patterning PDMS using a combination of wet and dry etching. *Journal of Micromechanics and Microengineering* 19, 047002.
59. Pasanen, T. P.; Laine, H. S.; Vähänissi, V.; Salo, K.; Husein, S., & Savin. H. (2018). Impact of standard cleaning on electrical and optical properties of phosphorus-doped black silicon. *IEEE Journal of Photovoltaics*, 8(3): 697–702.
60. Wilson, M., Lagowski, J., Jastrzebski, L., Savtchouk, A., & Faifer, V. (2001). COCOS (corona oxide characterization of semiconductor) non-contact metrology for gate dielectrics. In *AIP Conference Proceedings* (Vol. 550, No. 1, pp. 220-225). AIP.
61. Sugimoto, F & Okamura, S. (1999). Adsorption behavior of organic contaminants on a silicon wafer surface. *Journal of the Electrochemical Society* 146 (7), 1725-2729.
62. Bao, Y.; Li, S.; von Gastrow, G.; Repo, P.; Savin, H.; & Putkonen, M. (2015). Effect of substrate pretreatments on the atomic layer deposited Al2O3 passivation quality. *Journal of Vacuum Science & Technology A* 33, 01A123
63. Yang, L. & Gan, C. E. Costing small cleanrooms. (2007). *Building and Environment* 42, 743-751.
64. Markarian, J. (2009). Back-to-basics: adding colour to plastics. *Plastics, Additives and Compounding* 11 (4): 12-15.
65. Charvat, R. A. (2005). *Coloring of Plastics: Fundamentals, 2nd edition*, John Wiley & Sons, Hoboken, NJ, USA. ISBN 9780471721581.
66. Anttila, O. J.; Tilli, M. V.; Schaekers, M. & Claeys, C. L. (1992). Effect of chemicals on metal contamination on silicon wafers. *Journal of Electrochemical Society* 139 (4): 1180-1185.
67. Wendt, H.; Cerva, H.; Lehmann, V. & Pamler, W. (1989). Impact of copper contamination on the quality of silicon oxides. *Journal of Applied Physics* 65, 2402.
68. Heikkinen I. T. S., Kauppinen, C., Liu Z., Asikainen S. M., Spoljaric S., Seppälä J. V., Savin, H., Pearce, J. M. (2018). Chemical compatibility of fused filament fabrication - based 3-D printed components with solutions commonly used in semiconductor wet processing, *Additive Manufacturing* 23:99-107.